



HAL
open science

Atom economical coupling of benzophenone and N-heterocyclic aromatics with SmI 2

Arnaud Jaoul, Yan Yang, Nicolas Casaretto, Carine Clavaguéra, Laurent Maron, Grégory Nocton

► **To cite this version:**

Arnaud Jaoul, Yan Yang, Nicolas Casaretto, Carine Clavaguéra, Laurent Maron, et al.. Atom economical coupling of benzophenone and N-heterocyclic aromatics with SmI 2. *Chemical Communications*, 2020, 10.1039/D0CC05164K . hal-02941564

HAL Id: hal-02941564

<https://hal.science/hal-02941564v1>

Submitted on 17 Sep 2020

HAL is a multi-disciplinary open access archive for the deposit and dissemination of scientific research documents, whether they are published or not. The documents may come from teaching and research institutions in France or abroad, or from public or private research centers.

L'archive ouverte pluridisciplinaire **HAL**, est destinée au dépôt et à la diffusion de documents scientifiques de niveau recherche, publiés ou non, émanant des établissements d'enseignement et de recherche français ou étrangers, des laboratoires publics ou privés.

Atom economical coupling of benzophenone and N-heterocyclic aromatics with SmI_2

Arnaud Jaoul,^a Yan Yang,^b Nicolas Casaretto,^a Carine Clavaguéra,^{c*} Laurent Maron^{b*} and Grégory Nocton^{a*}

a. LCM, CNRS, Ecole polytechnique, Institut polytechnique Paris, Route de Saclay, 91128 Palaiseau, France.

b. LPCNO, UMR 5215, Université de Toulouse-CNRS, INSA, UPS, Toulouse, France

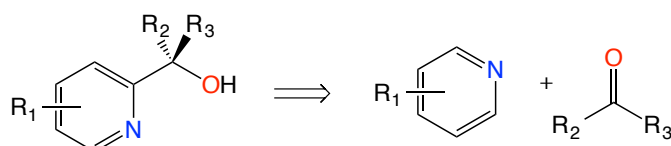
c. Université Paris-Saclay, CNRS, Institut de Chimie Physique, UMR8000, 91405 Orsay, France

Abstract: The use of stoichiometric SmI_2 in combination with benzophenone and N-heterocyclic aromatics such as bipyridine, phenanthroline and neat pyridine allows the direct ortho-coupling of both partners in an atom economical reaction free of any other coupling additives. The transformation was investigated by ^1H NMR, X-ray studies and theoretical calculations providing reaction intermediates and the reaction mechanism.

The substitution of pyridine-based heteroarenes is an important area of research considering the numerous applications of such compounds in pharmaceutical, agrochemical, materials and organometallic chemistry, in which they are common ligand motifs.¹⁻³ Originally, the general synthetic scheme for the substitution of aromatics lied in the Friedel-Crafts alkylation or acylation (electrophilic aromatic substitution) using strong Lewis acids, which is more difficult for neat pyridine.⁴⁻⁶ The acylation is particularly well adapted for the preparation of aryl ketones, which can be further reduced in alcohol or alkanes via adapted methods, but suffers from the use of high energy electrophiles.⁷

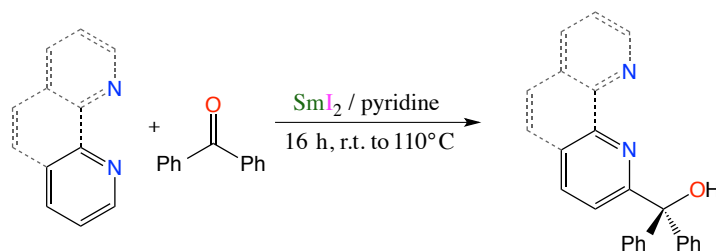
With heteroaromatics, traditional electrophilic aromatic substitutions are also well documented and usually involve a first step of C-H or C-X activation with strong bases or reducing metals (Li, Zn, Mg),⁸⁻¹⁰ followed by the addition of an electrophile, or the use of regioselective coupling catalysts such as palladium,^{2, 11} rhodium,¹² or iridium metal complexes.¹³ Alternatively, radical reactions are used such as the Minisci-type reactions.¹⁴ However, these radical reactions have limitations, especially in the regioselectivity of the products and the moderate yields.¹⁵

One important aspect of this peculiar chemistry lies in the preparation of α -substituted pyridinemethanols (carbinols) from pyridine and various ketones (Scheme 1),¹⁶ which originally employed either aluminium or magnesium in combination with mercuric chloride and iodine or a mixture of Hg/HgCl.¹⁷ Greener alternatives for carbinol syntheses are reported from aldehydes using strong Lewis acids but prevent the synthesis of tertiary alcohols.¹⁶



Scheme 1. General strategy for the synthesis of α -substituted pyridinemethanols (carbinols).

Additionally, the seminal work by Helquist and co-workers focalized on the coupling of various ketones and several N-aromatic heterocycles, notably phenanthroline and bipyridine, using a simple divalent halide, SmI₂.^{18, 19} In this article, we propose insights in the mechanism of such a reaction that we were able to extend to neat pyridine with benzophenone, yielding the corresponding bisphenylpyridyl alcohol (Scheme 2).



Scheme 2. Direct coupling of benzophenone and pyridine, bipyridine and phenanthroline with SmI₂.

Divalent samarium halides are well-known single electron transfer reagents in organic chemistry.²⁰⁻²⁵ In particular, Kagan reported the reaction of ketones for the preparation of alcohols or pinacols, depending upon the reaction conditions.²⁶ After some of us demonstrated that this typical radical coupling induced by divalent lanthanides was reversible in multiple cases,²⁷⁻³⁰ we were interested in investigating the Kagan reaction with benzophenone and SmI₂ in THF.

The reaction with 1 eq. of SmI₂ and benzophenone in anhydrous THF led to the fast formation of a white precipitate, poorly soluble in THF, which can be crystallized from hot THF and analyzed by X-ray diffraction, confirming the pinacol form of the product (**1**).³¹ In **1**, each samarium ion is coordinated by two iodide ions and three THF molecules (See SI) in a distorted square pyramidal fashion. The Sm-I average distance is 3.10(1) Å while the Sm-O(THF) and the Sm-O(alcoholate) are 2.44(5) and 2.075(12) Å, respectively. The carbon-carbon distance between the two Ph₂CO motifs is 1.56(3) Å and is indicative of a single bond. It is informative to compare this solid-state structure to the bridged structure that was proposed by Hoz in THF

solution by stopped-flow kinetics.³² However, the solid-state structure does not necessarily reflect the solution speciation.

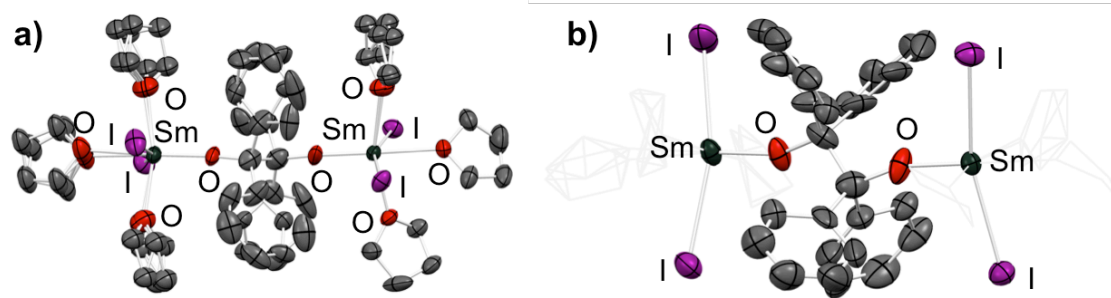
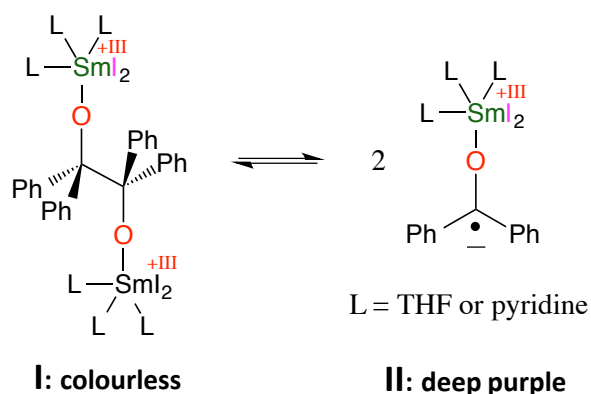


Figure 1. ORTEP of **1**. Thermal ellipsoids are at 50% level. 1a and 1b are two different views. In 1b, the thf are shown in light grey wireframes.

Along the communication, Arabic numbers are for solid-state compounds, capital Latin numbers for solution structures and capital alphabetical letters for computed gas phase compounds. When a suspension of **1** is prepared in THF-*d*₈ (**I**) and heated, the colour of the solution turns purple in good agreement with the formation of a ketyl radical. Visible spectroscopy was performed at various temperatures and showed an evolution upon heating of the band at 575 nm, which is attributed to the $\pi^* \rightarrow \pi^*$ transition of the charge-separated ketyl radical (**II**) (Scheme 3, Figure S15).³³ The colour change is reversible upon lowering the temperature. The low solubility of the dimeric form at room temperature prevented us to follow quantitatively the equilibrium by ¹H NMR studies.

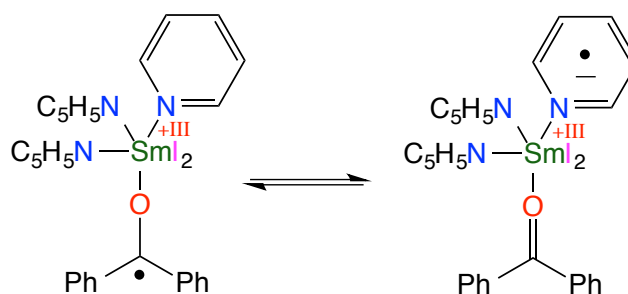


Scheme 3. Reversible coupling of benzophenone with $\text{SmI}_2(\text{L})_3$ fragments (L= pyridine or THF).

The white crystals of **1** can be dissolved in pyridine to yield an immediate colour change, the solution turning to deep purple, in agreement with the ketyl radical form of the benzophenone (**II**). The visible spectrum highlights a transition at 575 nm, similar to that of **I** at higher temperature (Figure S13). The ¹H NMR spectrum contains several broad signals, in agreement with the presence of paramagnetic species but remains difficult to assign. The ketyl radical (**II**) was found to be stable over several weeks in pyridine solutions at room temperature. At lower temperatures, the purple colour turns to blue and then to yellow at -40 °C. The band at 575 nm disappears and the visible spectrum becomes similar to that of **I** at room temperature (Figure S14).

As shown in the crystal structure of **1** (Figure 1), the solvent also acts as a ligand, completing the coordination sphere of the samarium ion. The THF is *s*-donating allowing the samarium to be more easily oxidized. Thus, the redox potential of the $\text{SmI}_2(\text{THF})_3(\text{benzophenone})$ fragment is lower than that of the $\text{SmI}_2(\text{pyr})_3(\text{benzophenone})$ fragment. Subsequently, the $\text{I} \rightleftharpoons \text{II}$ equilibrium is strongly displaced toward the monomeric form (**II**) in pyridine at room temperature and lower temperatures (-40 °C) are needed to favour **I**. These observations are in good agreement with previous work on the reversibility of these radical coupling reactions.^{27, 28}

When a solution of **II** was heated up to 100 °C, new features appeared in the visible spectrum, in particular around 475 and 700 nm. Both of these features are characteristic of SmI₂ in neat pyridine (Figure S13). According to the literature, SmI₂ is capable of reducing pyridine (**III**),³⁴ which probably allows the displacement of another equilibrium at higher temperature (Scheme 4).



Scheme 4. Electron transfer from the benzophenone to the pyridine in SmI₂(pyr)₃(benzophenone).

With this information in hand, we could now evaluate the equilibrium of the ketyl radical over other p-accepting N-heteroaromatics such as bipyridine (bipy) or phenanthroline (phen) with higher reduction potentials than pyridine. The addition of one equivalent of bipy or phen to a room temperature purple solution of **II** in pyridine led to a slight colour change to dark brown. These solutions faded to lighter brown, orange and yellow in a period of time of 16 h, indicating a degradation of the ketyl radical (**II**). The crystallization at cold of both solutions (-40 °C) produced pale yellow X-ray suitable crystals of **2** (bipyridine) and **3** (phenanthroline, Figure 2, Table 1), in which the benzophenone has been reduced to an alcoholate and is linked to the bipyridine and phenanthroline in the α-position to the nitrogen (Scheme 2, Figure 2), similar to what Helquist reported.^{18, 19} In **2**, one residual neutral bipyridine coordinates while in **3** three solvent molecules are coordinated to the samarium ion, which is then octa-coordinated by two iodide atoms and the novel tridentate ligand. The Sm-I distances are 3.288(1) and 3.23(5) Å in **2** and **3**, respectively, in good agreement with the presence of a trivalent samarium.³⁵ The C(Ph₂)-O distances of 1.38(1) and 1.395(7) Å in **2** and **3** agree with an alcoholate form. The OCCN torsion angle is small two very different sets of Sm-N distances are noted.

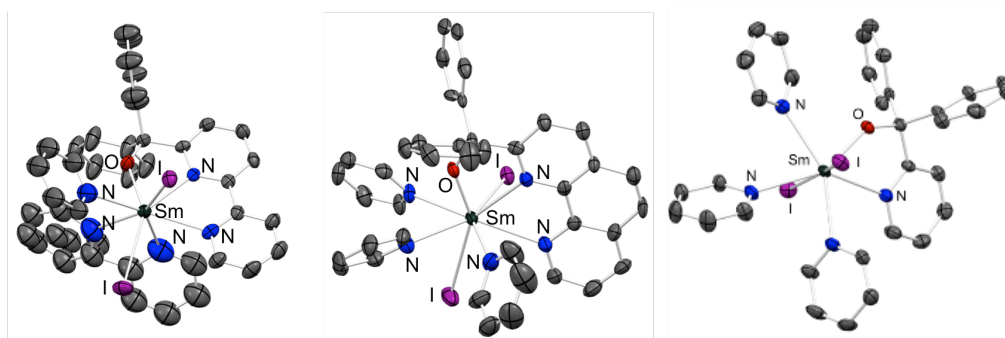


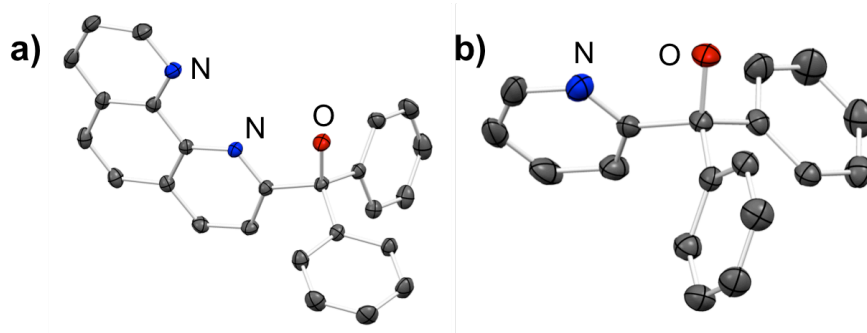
Figure 2. ORTEPs of **2-4** (from left to right). Thermal ellipsoids are at 50% level.

The reactivity clearly resembles the preparation of carbinols from pyridine and ketones but without the use of mercuric chloride¹⁷ or any coupling additives other than SmI₂, a much cleaner and atom economical pathway, as reported by Helquist.^{18, 19} However, the useful reaction was not reported with neat pyridine and although this reactivity does not happen at room temperature with neat pyridine, a solution of **II** was heated at 110 °C for 16 h and turned yellow. The yellow solution was crystallized and X-ray suitable colourless crystals of **4** were obtained (Figure 2, Table 1). The overall arrangement is similar to that in **2** and **3** with a newly-formed bidentate NO ligand, two iodides and three pyridine molecules coordinated to the Sm atom. Noticeably shorter Sm-I and Sm-N(pyr) distances are observed due to the smaller coordination number.

Table 1. Main distances and angles in **2-4**.

	SmI ₂ (py) ₅ ³⁵	2 (bipy)	3 (phen)	4 (pyridine)
Sm-I	3.288(1)	3.208(6)	3.23(5)	3.12(2)
Sm-N(pyr)	2.70(1)	3.70(1)	2.67(4)	2.62(6)
Sm-N(L)	-	2.556(9)	2.56(2)	2.568(4)
		2.654(10)	2.70(2)	
Sm-O	-	2.145(8)	2.15(2)	2.128(3)
O-C(Ph ₂)	-	1.38(1)	1.395(7)	1.395(6)
C-C(Ph ₂)	-	1.52(2)	1.54(1)	1.545(7)
OCCN	-	7.3	5.6(8)	3.6

The syntheses of the compounds **5** and **6** are performed in pyridine in one pot with one equivalent of SmI₂, benzophenone and bipyridine or phenanthroline, respectively. The synthesis of **7** is also performed in pyridine. After acidic treatment and purification by re-crystallization, **6** and **7** are obtained as white powders in 70-75% yield, while **5** is obtained as an oil.

**Figure 3.** ORTEPs of **6** and **7** (from left to right). Thermal ellipsoids are at 50% level.

In order to get further insights in the reaction mechanism of these important transformations, theoretical computations at the DFT level (B3PW91) were performed. The formation of a ketyl radical was already investigated by Zhao *et al.*³⁶, Kefalidis *et al.*³⁷ or Werner *et al.*³⁸ and therefore its formation was not investigated computationally in this report. The nature of the equilibrium depicted in scheme 4 was investigated computationally for pyridine and phenanthroline. In compound **B**, the ketyl radical appears to be favoured by 7.8 kcal/mol over the phenanthroline radical, whereas the preference for the ketyl radical is 12.7 kcal/mol in comparison with the pyridine radical (see SI). This is in agreement with a higher π^* energy for pyridine compared to phenanthroline. A plausible mechanism for the formation of **D** (**2** in the solid-state) from the coupling between the ketyl radical and phenanthroline/pyridine was determined computationally (Figure 4). The formation of the ketyl radical is favoured by 7.6 kcal/mol but the coordination of the phenanthroline does not imply any electron transfer from the ketyl radical to the phenanthroline moiety, in agreement with the computed 7.8 kcal/mol needed to achieve this transfer. The unpaired electron is mainly located on the oxygen and the carbon atoms of the ketyl (see figure 4 and ESI). The system reaches an accessible C-C coupling transition state (barrier of 18.5 kcal/mol). The C-C bond is developing between the ketyl carbon atom that bears unpaired spin density and the carbon in alpha to the nitrogen of phenanthroline. The latter position is imposed by the *cis*-coordination of the phenanthroline to the samarium centre through the two nitrogen lone pairs. This TS is described as a radical coupling reaction because the unpaired electron of the ketyl radical couples with the π electron of alpha carbon of the phenanthroline ligand, explaining the height of the barrier. Following the intrinsic reaction coordinate, it yields the alcoholate intermediate (**C**) whose formation is endothermic by 8.8 kcal/mol from the ketyl radical form. This is due to the formation of an sp^3 carbon on bipyridine inducing a loss in aromaticity.

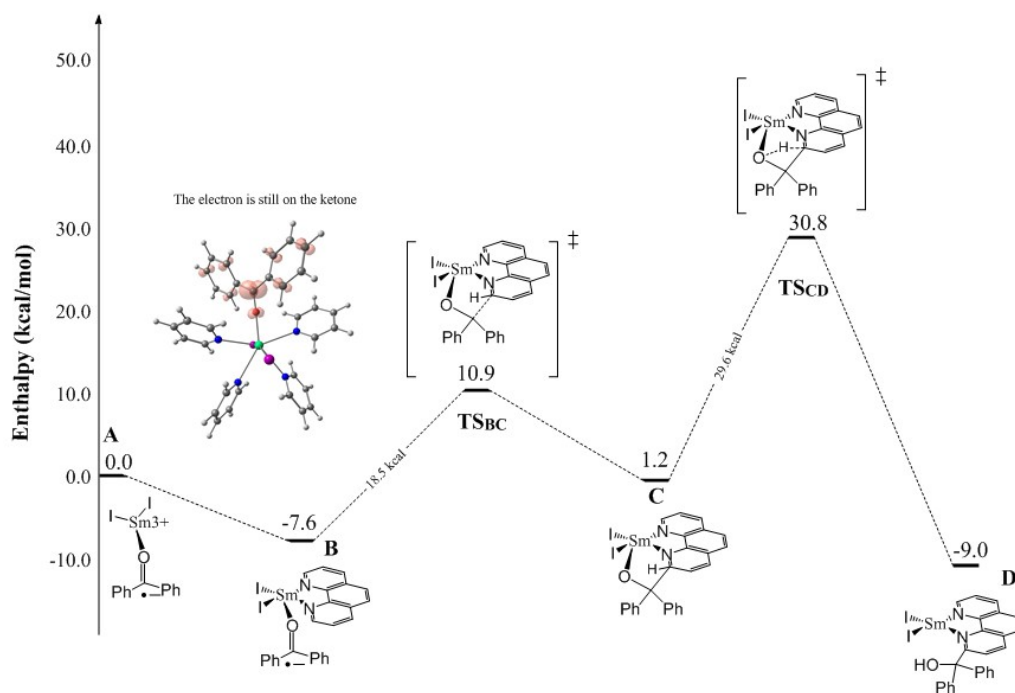


Figure 4. Computed enthalpy profile at room temperature for the formation of **2** from the coupling between **II** and phenanthroline

At this stage, the intermediate (**C**) can further evolve in order to retrieve the aromaticity of the phenanthroline by undergoing an intramolecular 1,3 proton shift in the alcoholate ligand. The associated barrier is 29.6 kcal/mol from **C** indicating a kinetically possible reaction and the rate-determining step of the process. The height of the barrier is due to the lack of samarium involvement in the proton transfer as well as the decrease of the Sm-O stabilizing interaction. This yields to **D**, whose formation is favoured by 9.0 kcal/mol from the entrance. Similar calculations were performed for the formation of the pyridine analogue (see ESI). The mechanism appears to be similar but all intermediates are shifted up in energy by up to 10.6 kcal/mol for the rate determining step TS and the final product formation. This is in line with the experimental observation that higher temperature is required to drive the reaction. The deprotonation of the alcohol is then assisted by the pyridine base as the solvent as well as by the coordination of the samarium ion.

In conclusion, this article reports the easy formation of carbinols from benzophenone and N-heterocycles, such as bipyridine, phenanthroline and even neat pyridine. The equilibrium between the ketyl radical and its coupled form (pinacolate) is the key step of this atom-economical method that allows direct radical coupling with the N-heterocycle followed by an intra-molecular hydrogen transfer without any other coupling additives. The mechanism was confirmed by theoretical computations and further work is being conducted to enlarge the scope of the reaction with substrates more difficult to reduce.

Conflicts of interest

There are no conflicts to declare.

Notes and references

1. Y. Fujiwara, J. A. Dixon, F. O'Hara, E. D. Funder, D. D. Dixon, R. A. Rodriguez, R. D. Baxter, B. Herlé, N. Sach, M. R. Collins, Y. Ishihara and P. S. Baran, *Nature*, 2012, **492**, 95-99.
2. P. Guo, J. M. Joo, S. Rakshit and D. Sames, *J. Am. Chem. Soc.*, 2011, **133**, 16338-16341.
3. M. Schlosser and F. Mongin, *Chem. Soc. Rev.*, 2007, **36**, 1161-1172.
4. C. M. Jephcott, *J. Am. Chem. Soc.*, 1928, **50**, 1189-1192.
5. N. O. Calloway, *Chem. Rev.*, 1935, **17**, 327-392.
6. P. H. Gore, *Chem. Rev.*, 1955, **55**, 229-281.
7. G. A. Olah, *Friedel-Crafts Chemistry*, Wiley, New York, 1973.

8. T. Bresser, G. Monzon, M. Mosrin and P. Knochel, *Organic Process Research & Development*, 2010, **14**, 1299-1303.
9. V. Snieckus, *Chem. Rev.*, 1990, **90**, 879-933.
10. K. R. Campos, *Chem. Soc. Rev.*, 2007, **36**, 1069-1084.
11. M. Ye, G.-L. Gao and J.-Q. Yu, *J. Am. Chem. Soc.*, 2011, **133**, 6964-6967.
12. J. C. Lewis, R. G. Bergman and J. A. Ellman, *J. Am. Chem. Soc.*, 2007, **129**, 5332-5333.
13. I. A. I. Mkhaliid, J. H. Barnard, T. B. Marder, J. M. Murphy and J. F. Hartwig, *Chem. Rev.*, 2010, **110**, 890-931.
14. M. A. J. Dunton, *Med. Chem. Comm.*, 2011, **2**, 1135-1161.
15. F. Minisci, E. Vismara and F. Fontana, *Heterocycles*, 1989, **28**, 489-519.
16. A. Harikrishnan, J. Sanjeevi and C. Ramaraj Ramanathan, *Org. Biomol. Chem.*, 2015, **13**, 3633-3647.
17. C. H. Tilford, R. S. Shelton and M. G. v. Campen, *J. Am. Chem. Soc.*, 1948, **70**, 4001-4009.
18. J. A. Weitgenant, J. D. Mortison, D. J. O'Neill, B. Mowery, A. Puranen and P. Helquist, *J. Org. Chem.*, 2004, **69**, 2809-2815.
19. J. A. Weitgenant, J. D. Mortison and P. Helquist, *Org. Lett.*, 2005, **7**, 3609-3612.
20. G. A. Molander and C. R. Harris, *Chem. Rev.*, 1996, **96**, 307-338.
21. K. C. Nicolaou, S. P. Ellery and J. S. Chen, *Angew. Chem. Int. Ed.*, 2009, **48**, 7140-7165.
22. M. Szostak, N. J. Fazakerley, D. Parmar and D. J. Procter, *Chem. Rev.*, 2014, **114**, 5959-6039.
23. X. Just-Baringo and D. J. Procter, *Acc. Chem. Res.*, 2015, **48**, 1263-1275.
24. C. Beemelmans and H.-U. Reissig, *Chem. Soc. Rev.*, 2011, **40**, 2199-2210.
25. S. Shi and M. Szostak, *Molecules*, 2017, **22**, 2018.
26. H. B. Kagan, *J. Alloys Compd.*, 2006, **408**, 421-426.
27. G. Nocton, W. L. Lukens, C. H. Booth, S. S. Rozenel, S. A. Melding, L. Maron and R. A. Andersen, *J. Am. Chem. Soc.*, 2014, **136**, 8626-8641.
28. G. Nocton and L. Ricard, *Chem. Commun.*, 2015, **51**, 3578-3581.
29. A. Jaoul, G. Nocton and C. Clavaguéra, *Chem. Phys. Chem.*, 2017, **18**, 2688-2696.
30. T. Cheisson, L. Ricard, F. W. Heinemann, K. Meyer, A. Auffrant and G. Nocton, *Inorg. Chem.*, 2018, **57**, 9230-9240.
31. P. Girard, R. Couffignal and H. B. Kagan, *Tet. Lett.*, 1981, **22**, 3959-3960.
32. H. Farran and S. Hoz, *J. Org. Chem.*, 2009, **74**, 2075-2079.
33. T. Shida, *Electronic absorption spectra of radical ions*, Elsevier Science Ltd., Amsterdam and New York, 1988.
34. Y. Kamochi and T. Kudo, *Heterocycles*, 1993, **36**, 2383-2396.
35. J. C. Berthet, P. Thuery and M. Ephritikhine, *CCDC 959301: Experimental Crystal Structure Determination*, 2013, DOI: 10.5517/cc11676p.
36. X. Zhao, L. Perrin, D. J. Procter and L. Maron, *Dalton Trans.*, 2016, **45**, 3706-3710.
37. C. E. Kefalidis, L. Perrin and L. Maron, *Eur. J. Inorg. Chem.*, 2013, **2013**, 4042-4049.
38. D. Werner, X. Zhao, S. P. Best, L. Maron, P. C. Junk and G. B. Deacon, *Chem. Eur. J.*, 2017, **23**, 2084-2102.